Freezing of Fluids Confined in a Disordered Nanoporous Structure

B. Coasne,[1] S. K. Jain,[2] and K. E. Gubbins[2]

[1]*Laboratoire de Physicochimie de la Matière Condensée, Université Montpellier 2 and CNRS (UMR 5617), Montpellier, France*
[2]*Center for High Performance Simulation and Department of Chemical and Biomolecular Engineering, North Carolina State University, Raleigh, North Carolina 27695, USA*

(Received 20 January 2006; published 8 September 2006)

Freezing of a simple fluid in a disordered nanoporous carbon is studied using molecular simulations. Only partial crystallization occurs, and the confined phase is composed of crystalline and amorphous nanodomains. This freezing behavior departs strongly from that for nanopores of simple geometry. We present a method for analyzing the freezing in such disordered materials in terms of a transition in the average size and number of crystalline clusters. The results provide a basis for the interpretation of experiments on freezing in such materials, particularly ^{1}H-NMR and scattering experiments.

DOI: 10.1103/PhysRevLett.97.105702 PACS numbers: 64.60.−i, 05.70.−a, 61.46.−w

Freezing and melting in nanoporous materials is of fundamental interest in understanding the effect of confinement, reduced dimension, and surface forces on the thermodynamics of fluids [1–5]. Shifts in the freezing temperature and, in some cases, new surface- or confinement-induced phases, are observed on reducing the width of the confined space to approach the range of the intermolecular forces [6,7]. Experimental, molecular simulation, and theoretical studies have shown that, for simple fluids and pore geometries, the freezing temperature can be described as a function of the reduced pore size $H^* = H/\sigma$ (H is the pore width and σ the diameter of adsorbate molecule) and the ratio of the wall-fluid (wf) to the fluid-fluid (ff) interactions, $\alpha \sim C\rho_w\varepsilon_{wf}/\varepsilon_{ff}$ [7], where ρ_w and ε are the density of wall atoms and the potential well depth, respectively, and C is a constant that depends on the wall geometry. The freezing temperature is decreased compared to the bulk for $\alpha < 1$, while it is increased for $\alpha > 1$ [8]. The magnitude of the shift in the transition temperature depends on H^*, while the appearance of surface or confinement driven phases usually depends on a combination of effects from α and H^* [9].

Experimental studies of freezing in nanoporous materials have been severely hampered by difficulty in the interpretation of the results. A change in some measured property (e.g., calorimetry, NMR, dielectric properties) is observed, but the presence of any phase transition, and the nature of the phases observed, is often the subject of controversy. Most simulation and theoretical studies have treated porous carbons as an assembly of independent, unconnected pores of simple slit geometry. In such studies, the nature of the phase transition and of the phases involved can be determined reliably, provided care is taken over finite size effects and free energy calculations. However, the question remains as to what relation such calculations bear, if any, to the experimental results, which are for materials with connected pores of varying geometry and size, rough surfaces, etc. It has been shown that capillary condensation (gas-liquid) in disordered porous structures differs significantly from that of simple systems [10–13]. In contrast, the effect of pore shape and connectivity on freezing of confined fluids has received very little attention [7,14]. The objective of the work reported here is to clarify the nature of freezing in one particular class of disordered nanoporous materials, namely, carbons, to suggest a new way to interpret experimental results, and to determine what, if any, relation such phenomena have to freezing in ideal slit pores.

Advances in modeling of disordered porous carbons have been achieved through the use of reverse Monte Carlo (RMC) methods [15]. Gubbins and coworkers [16,17] have shown that the structural models obtained using RMC simulations with appropriate three-body constraints are in good agreement with experimental data from transmission electronic microscopy, gas adsorption, and calorimetry [16]. In this Letter, we report a simulation study of freezing of Ar in such a realistic model of disordered porous carbons. We also consider freezing in an ordered model of porous carbons (slit pores) and compare this with the freezing in the disordered material.

The disordered porous carbon used in this work is shown in Fig. 1. The pore size distribution of the material shows a mean value of ~11 Å with a dispersion of ±4 Å. This structural model of saccharose-based carbon was obtained using a constrained RMC technique [17], which consists of generating atomic configurations that match the pair correlation function of the real system. Two other constraints were simultaneously minimized in the simulation to account for three-body forces: (i) The fraction of 3-coordinated C atoms must be equal to that determined from experiment, and (ii) the average C-C-C bond angle must be distributed about $2\pi/3$ (sp^2 hybridization). The sampling in the RMC simulations was improved by combining the method with a simulated annealing technique [16]. Freezing of Ar was also studied for the slit pore model. Three pore sizes $H = 7$, 11, and 14 Å were selected as they correspond to the smallest, mean, and largest pore sizes of the disordered carbon, respectively.

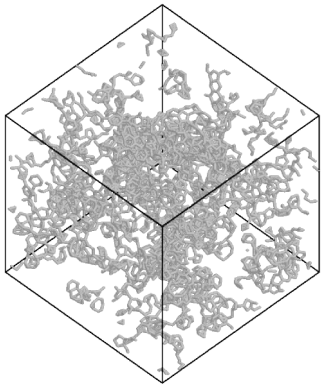

FIG. 1. Structural model of a disordered porous carbon obtained using a constrained reverse Monte Carlo method. The box size is 5 nm. The gray sticks represent the C-C bonds.

Freezing of the confined fluid was simulated in both the slit pores and the disordered carbon using Monte Carlo simulations in the grand canonical ensemble (μ, V, T) [18]. Simulations were performed for several temperatures at a chemical potential corresponding to that of an ideal gas at a pressure of 1 atm. Periodic boundary conditions were applied to avoid surface effects. The interaction of Ar with the C atoms of the disordered material was modeled using a Lennard-Jones (LJ) potential. The interaction between Ar and each slit pore wall was calculated using the 10-4-3 Steele potential [7]; this potential corresponds to the integration of the Ar/C LJ potential over each C atom of an infinite graphite plane, followed by summation over an infinite number of planes. The use of the Steele potential, which neglects the effect of surface corrugation, is expected to be a reasonable approximation as the size for Ar (~3.4 Å) is much larger than the C-C bond length in graphite (~1.4 Å). The fluid-fluid ($\sigma = 3.405$ Å, $\varepsilon = 120$ K) and fluid-wall ($\sigma = 3.38$ Å, $\varepsilon = 58$ K) parameters were the same for both pore models. To circumvent the difficulty of particle deletion and insertion in dense phases, the simulations were combined with the parallel tempering technique, which prevents the system from being ''trapped'' in local metastable states.

Strong layering of Ar in the slit pores was observed due to the interaction with the pore walls; 2D layers are separated by a minimum value of the density $\rho^* \sim 0$. The slit pores $H = 7$, 11, and 14 Å accommodate 1, 2, and 3 layers, respectively. Freezing of Ar in these slit pores was studied by analyzing for each layer in-plane 2D positional and bond-orientational pair correlation functions and bond-order parameters [18]. For a given pore size, all the confined layers freeze at the same temperature. In the frozen phase, these layers have a hexagonal crystal structure (triangular symmetry) with, however, some defects. The freezing temperature of Ar in the slit pores ($T = 140$, 116, and 112 K for $H = 7$, 11, and 14 Å, respectively) was found to be much larger than that of bulk Ar ($T = 83$ K). This increase in the freezing temperature was expected, as we know from previous experimental and theoretical works that fluids in strongly attractive pores crystallize at higher temperature than the bulk [7,8]. It is also found that the shift in the freezing temperature becomes larger as the pore size decreases, as expected.

The density of Ar in the disordered carbon is shown in Fig. 2 as a function of the temperature T. A change in the evolution of the density with T is observed for $T \sim 115$ K; ρ^* is almost constant at about 0.4–0.5 for $T < 115$ K, while ρ^* decreases more rapidly with increasing T for $T > 115$ K. As shown in Fig. 2, this change in the variation of the density at $T \sim 115$ K is accompanied by a decrease from 11.1 to 9.6 kJ/mol of the isosteric heat of adsorption Q_{st}. The changes in ρ^* and Q_{st} indicate that Ar confined within the disordered porous carbon undergoes modifications at $T \sim 115$ K. Interestingly, this temperature is very close to the freezing temperature for the slit pore with $H = 11$ Å, which corresponds to the mean pore size of the disordered porous structure. This result suggests that the freezing behavior of Ar in the complex carbon is driven by the mean pore size.

The pair correlation function $g(r)$ of Ar in the disordered carbon was calculated for each temperature (Fig. 3). For the disordered carbon at all temperatures, the $g(r)$ function is characteristic of liquidlike structures, with only short-range positional order observed. The maximum value of the $g(r)$ function, which corresponds to the amplitude of the nearest neighbor peak, is reported in Fig. 4 as a function of T. The maximum value is constant at about $g_{max} = 3$ for $T > 115$ K; this value is close to that expected for a bulk fluid. On the other hand, g_{max} increases linearly with decreasing T for $T < 115$ K. Such an analysis indicates that short-range structural changes of Ar in the disordered carbon occur at $T \sim 115$ K. The augmentation in g_{max} with decreasing T indicates that the confined phase presents more short-range order for $T < 115$ K, although it remains liquidlike overall. A criterion to demonstrate the existence of a solid phase has been proposed by Hansen and Verlet [19]. The amplitude of the first peak $S(k_0)$ of the structure factor can be as high as 2.85 for an isotropic phase and 5.0

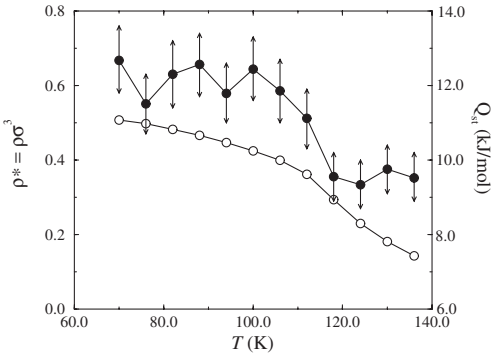

FIG. 2. Density ρ^* (○, left axis) and isosteric heat Q_{st} (●, right axis) for Ar in the disordered carbon as a function of T.

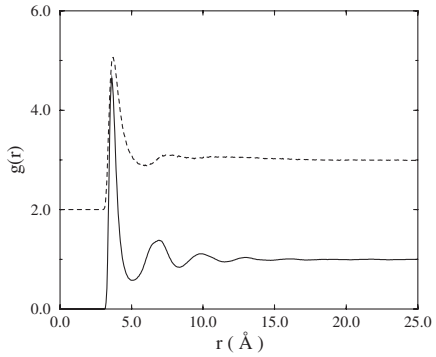

FIG. 3. Pair correlation function $g(r)$ for Ar in the disordered carbon at $T = 70$ K (solid line) and $T = 136$ K (dashed line). The $g(r)$ function for $T = 136$ K has been shifted by $+2.0$.

for a 2D phase [7]; higher values indicate a solid phase. We checked that $S(k_0)$ for Ar in the disordered carbon is always lower than 2.85, which confirms that the fluid remains liquidlike even at the lowest temperature.

The structure of Ar in the disordered carbon was further characterized by determining the degree of crystalline order as a function of T. Global order parameters are not suitable to study freezing in the complex carbon as the large degree of disorder of the sample prevents a coherent positional and orientational order of the confined phase. Instead of global parameters, we used a local order parameter proposed by Ten Wolde *et al.* [20] to calculate the percentage of atoms in a crystal-like state. For each atom i of the confined phase, we calculated the 13 normalized parameters $\tilde{q}_{6m}(i)$ that are defined as:

$$\tilde{q}_{6m}(i) = \frac{A}{N_b(i)} \sum_{j=1}^{N_b(i)} Y_{6m}(\mathbf{r}_{ij}) \quad \text{with } m \in [-6, 6], \qquad (1)$$

where $\mathbf{r}_{ij}$ are the vectors joining the atom i and each of its $N_b(i)$ neighbors j. Y_{6m} are spherical harmonics and A is the normalization constant. $\tilde{q}_{6m}(i)$ is a local quantity that depends only on i and its neighbors j. For each pair of nearest neighbors, we define the scalar product [20]:

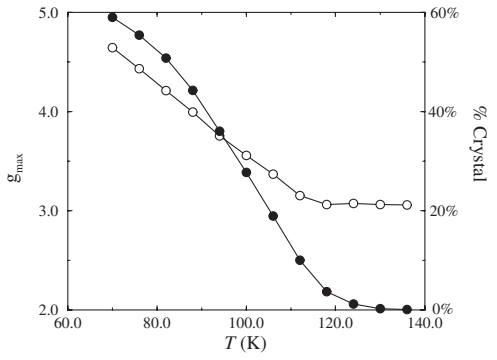

FIG. 4. Maximum value (first peak) of the function $g(r)$ (○, left axis) and percentage of crystal-like atoms (●, right axis) as a function of the temperature for Ar in the disordered carbon.

$$\mathbf{q}_6(i) \cdot \mathbf{q}_6(j) = \sum_{m=6}^{m=-6} \tilde{q}_{6m}(i)\tilde{q}_{6m}(j)^*. \qquad (2)$$

Atoms i and j can be considered "connected" in a coherent manner if $\mathbf{q}_6(i) \cdot \mathbf{q}_6(j) \geq 0.5$. Ten Wolde *et al.* have shown that i is crystal-like if it is connected in a coherent manner to at least 7 of its nearest neighbors; this definition ensures that liquid and crystal structures are unambiguously distinguished. As shown in Fig. 4, the fraction of crystal-like atoms increases in a continuous way from 0% for $T >$ 115 K up to 60% for $T \sim 70$ K. By contrast, for the slit pore there is an abrupt change on melting in the number of crystal-like atoms, as indicated by the order parameter analysis. The results in Fig. 4 show that the phase in the disordered carbon for $T < 115$ K is a mixture of crystalline clusters and amorphous (liquid or solid) regions. Such an observation is supported by experiments on fluids in silica pores, which have shown that the confined fluid does not crystallize but forms an inhomogeneous phase composed of nanoscopic crystallites and amorphous regions [21,22].

The structure of Ar in the disordered carbon was characterized in a more complete way by performing a cluster analysis as a function of T. The distribution of the number of connections per Ar atom was calculated for each temperature from the number of nearest neighbor bonds for which $\mathbf{q}_6(i) \cdot \mathbf{q}_6(j) \geq 0.5$. For all temperatures, the confined phase is composed of both crystal (number of connections >7) and liquid (number of connections <7) adsorbed atoms. The average number of connections per atom decreases on increasing T from 6.9 at $T = 70$ K down to 1.7 at $T = 136$ K. Even at low temperature, the average number of connections per atom is much lower than the values expected for fcc and bcc bulk crystals (number of connections ~12 and 13, respectively [20]). This result is due to the confinement and the disorder of the porous material, which prevent the formation of any bulklike regular crystal. This finding strongly departs from what is observed for the slit geometry, where the pore accommodates layers of an adsorbate having a well-defined crystalline structure. The size distribution of crystalline clusters in the disordered carbon was also calculated for each temperature. The size distributions for $T < 106$ K have two peaks, with the confined phase being made up of large clusters of a few hundreds atoms and small clusters of less than 50 atoms. The fraction of small clusters increases with increasing T. On the other hand, the size distribution of crystalline clusters for $T \geq 106$ K has only one peak, which corresponds to small clusters of less than 200 atoms. The existence of the two different regimes, i.e., two peak vs. one peak distribution, can be seen as a percolation effect. For $T \geq 106$ K, crystal-like particles, which correspond to less than 20% of the atoms, form small clusters that are not connected; the average size of the crystalline clusters increases with decreasing T, due to the increase in the number of crystal-like atoms. For $T < 106$ K, some of

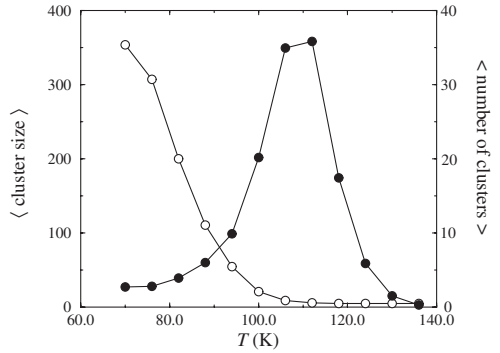

FIG. 5. Average size (○, left axis) and number (●, right axis) of crystalline clusters versus T for Ar in the disordered carbon.

the small clusters merge and form larger clusters (several hundred atoms). This analysis was confirmed by visualization of the configurations of Ar in the porous carbon.

The average size and number of Ar crystalline clusters in the disordered carbon is shown in Fig. 5 as a function of T. The average cluster size decreases with increasing T from $\sim$350 at $T = 70$ K down to 0–10 atoms for $T \geq 106$ K. In connection with the analysis of the average cluster size, we note that for $T < 106$ K the size distribution has two peaks. On the other hand, the average number of crystalline clusters as a function of T has a nonmonotonic behavior (Fig. 5), which provides insights into the structure of Ar in the disordered carbon. For $T \leq 112$ K, the number of clusters increases with increasing T; large clusters separate into small unconnected clusters as the number of crystal-like atoms decreases as T increases. For $T \leq 112$ K, there is a direct correlation between the average cluster size and number; the number of crystalline clusters increases as they become smaller. In contrast, the number of crystalline clusters for $T > 112$ K decreases with increasing T; less and less crystalline clusters can form when the T increases due to the decrease in the number of Ar crystal-like particles (as shown in Fig. 4, the percentage of crystal-like atoms decreases from $\sim$10% at $T = 112$ K down to 0% at $T = 136$ K). These last results indicate that the evolution with T of the average number and size of Ar crystalline clusters is modified at $T \sim 112$ K. This change in the behavior of the adsorbate in the disordered carbon explains the variation of density, isosteric heat, and correlation functions observed in Figs. 2 and 3. The results above show that the number of crystalline clusters is a key parameter in describing the solidification in a disordered material.

The present study shows that freezing of a simple fluid in a disordered porous structure strongly departs from that for unconnected slit pores of a simple geometry, with the low temperature phase being composed of crystalline and amorphous nanodomains in disordered materials. The present work shows that the properties of the confined phase can be understood by analyzing the distribution of crystal-like cluster size and number. These results provide a basis for the interpretation of experiments on freezing in disordered materials. ^{1}H-NMR and neutron scattering experiments could be used to estimate the proportion of liquid or solid particles and to check the existence of crystal clusters in the confined phase.

We thank C. Alba-Simionesco, G. Dosseh, F. R. Hung, R. J. M. Pellenq, and J. Teixeira for fruitful discussions. We thank the National Science Foundation (Grant No. CTS-0211792) and the U.S. Department of Energy (Grant No. DE-FG02-98ER14847) for support of this research.

[1] D. E. Silva, P. E. Sokol, and S. N. Ehrlich, Phys. Rev. Lett. **88**, 155701 (2002).
[2] J. Day, T. Herman, and J. Beamish, Phys. Rev. Lett. **95**, 035301 (2005).
[3] J. V. Pearce *et al.*, Phys. Rev. Lett. **95**, 185302 (2005).
[4] D. Wallacher and K. Knorr, Phys. Rev. B **63**, 104202 (2001).
[5] V. P. Soprunyuk *et al.*, Phys. Rev. B **67**, 144105 (2003).
[6] M. Alcoutlabi and G. B. McKenna, J. Phys. Condens. Matter **17**, R461 (2005).
[7] C. Alba *et al.*, J. Phys. Condens. Matter **18**, R15 (2006).
[8] R. Radhakrishnan, K. E. Gubbins, and M. Sliwinska-Bartkowiak, J. Chem. Phys. **116**, 1147 (2002).
[9] R. Radhakrishnan, K. E. Gubbins, and M. Sliwinska-Bartkowiak, Phys. Rev. Lett. **89**, 076101 (2002).
[10] E. Kierlik *et al.*, Phys. Rev. Lett. **87**, 055701 (2001).
[11] H. J. Woo and P. A. Monson, Phys. Rev. E **67**, 041207 (2003).
[12] R. J. M. Pellenq and P. E. Levitz, Mol. Phys. **100**, 2059 (2002).
[13] R. Salazar and L. D. Gelb, Phys. Rev. E **71**, 041502 (2005).
[14] M. J. Biggs, A. Buts, and D. Williamson, Langmuir **20**, 5786 (2004).
[15] R. L. McGreevy and L. Pusztai, Mol. Simul. **1**, 359 (1988).
[16] J. P. Pikunic *et al.*, Langmuir **19**, 8565 (2003).
[17] S. K. Jain *et al.*, Adsorption **11**, 355 (2005).
[18] B. Coasne *et al.*, Mol. Phys. **102**, 2149 (2004).
[19] J. P. Hansen and L. Verlet, Phys. Rev. **184**, 151 (1969).
[20] P. R. Ten Wolde, M. J. Ruiz-Montero, and D. J. Frenkel, J. Chem. Phys. **104**, 9932 (1996).
[21] M. Sliwinska-Bartkowiak *et al.*, J. Chem. Phys. **114**, 950 (2001).
[22] K. Morishige and H. Iwasaki, Langmuir **19**, 2808 (2003).